The Missing Cool Corona in the Flat Magnetic Field Around Solar Active Regions

THE UNIVERSITY OF ALABAMA IN HUNTSVILLE

Talwinder Singh[1], Alphonse Sterling[2] , Ron Moore[1]

[1] *Center for Space Plasma and Aeronomic Research (CSPAR), The University of Alabama in Huntsville, Huntsville, AL, USA*

[2] *NASA Marshall Space Flight Center, Huntsville, AL, USA*

DEPARTMENT OF SPACE SCIENCE
THE UNIVERSITY OF ALABAMA IN HUNTSVILLE

Introduction

- The Atmospheric Imaging Assembly (AIA) (Lemen et al 2012) onboard the Solar Dynamics Observatory (SDO) (Pesnell et al 2012) observes the corona in seven different EUV channels. The channels and their respective approximate peak coronal log10 temperature values being 304 A (4.7), 171 A (5.8), 193 A (6.2), 211 A (6.3), 131 A (5.6), 94 A (6.8), and 335 A (6.4).
- We observed that in some channels, with the primary one seeming to be 171 A, that ARs on the visible disk frequently are surrounded by an annular darker moat-like region, with the AR emitting brightly interior to that annulus, and with the quiet Sun emitting with brightness typical of the quiet Sun in regions exterior to that annulus. An example of this phenomenon is shown in Figure 1, with NOAA AR 12699 on 11 Feb 2018.
- In this study, we examine ARs that are isolated on the Sun, when they are near the center of the disk. This allows us to show clearly the moat-like regions of missing "cool" corona around the ARs and allows for more accurate AR magnetic flux measurements in our analysis since the LOS magnetograms lose their accuracy away from the solar disk center. Table 1 gives the dates of observations used in this work, along with the NOAA AR numbers of the active regions under consideration.
- Here, we study in more detail the thermal properties of the dark moat regions and argue that a moat forms when loops rooted in these regions, along with the lowest of the AR's own loops over these regions, are pushed down to low-enough heights by the overlying strong magnetic field that loops out from the AR (Singh et al 2021).

Moat properties

- To quantify the emission differences between moat and non-moat regions in different wavelengths, we find the average emissions in these regions for all 7 cases in Table 1. The external non-moat region is the surrounding area outside this manually selected moat region, and largely consists of quiet Sun. The outer moat boundaries for cases 1 to 7 can be seen in the Figures 2 and 3. These values show that, on average, the moat regions are significantly darker in 171 A and 131 A, they are comparable in intensity to non-moat regions in 304 A, 95 A, and 335 A, and are brighter in 193 A and 211 A wavelengths.
- From the images of the moats for 7 different cases, we can see that moats vary greatly in shape and size for the different ARs, and they often are not symmetric.
- We can quantitatively examine the distribution with temperature of the plasma along the line of sight from the observer through any imaged solar feature, by estimating the differential emission measure (DEM) function (Withbroe et al 1978, Boerner et al 2012). Figure 4 shows EM maps for the AR of Table 1 case 1, with the different panels showing the total EM contained within the specified temperature ranges. The dark moat visible in AIA 171 image of case 1 is most clearly seen in the log temperature range 5.75 to 6.05, consistent with the coronal emission being greatly suppressed in the dark moat in this temperature range.
- Figure 5 displays similar EM maps for Table 1 cases 2 to 7 in this same temperature range (log (T)=[5.75,6.05]). In each of these cases, the dark moat shows substantial EM depletion, consistent with the visual appearance in AIA 171 images.

Plausible explanation

- Antiochos et al 1986 explain the structure of the static corona by pointing out that there are two possible models for coronal loops: (1) a hot-loop model and (2) a cool-loop model; respectively yielding loops of temperature >10^5 K, and between about 2x10^4 and 10^5 K. They argued that the hot solution only works on loops with heights of >5000 km; If the loops have top heights less than ~5000 km they are restricted to temperatures only in the range of about 2x10^4 and 10^5 K.
- Because the moats have a propensity to be dark in only the cooler-temperature AIA channels, we suspect that coronal loops that would normally emit largely in the temperature range ~0.5--1.0 MK get flattened to heights less than ~5000 km, meaning that the hot solution stops working for them and only the cool solution of Antiochos et al 1986 is available. Thus, if the loops in the outskirts of ARs that would normally emit in this ~0.5--1.0~MK range, in particular the loops that would normally emit in the AIA 171 A band, are flattened to low heights, then this could explain why such regions are dark in images taken with filters sensitive to such wavelengths. Such flattened loops would tend to have temperatures below 10^5 K, and therefore they would tend to be dark in emission from plasma that emits in the AIA 171 A band.
- To examine the plausibility of this claim, we estimate the region around the ARs where the field pressure of the overlying splay of magnetic field from the AR is sufficient to suppress the heights of coronal loops in those surrounding regions. In order to suppress those surrounding loops, the magnetic pressure of the AR's outskirt field over the moat regions should be higher than beyond the non-moat regions and the moat boundaries should mark where the magnetic pressure has weakened to comparable to the magnetic pressure at the base of the corona in the quiet sun regions outside the moat. The magnetic pressure at ~20,000 km above the photosphere, calculated from the PFSS solution is shown for cases 1-7 in the Figures 6 and 7.
- We can see that the moat boundaries encapsulates a high magnetic pressure region, relative to the non-moat regions. Although the boundaries do not match exactly, there is obvious correlation between the dark moat region in AIA 171 A images and the high-pressure region in the PFSS solutions. The minor mismatches might be due to our potential field approximation of the coronal magnetic field or errors in visual estimation of the moat boundaries from AIA 171 A data. Overall, however, we regard the match as good enough to render plausible the idea that a moat region around ARs is often dark in 171 A and similar wavelengths because the strong AR field pushes down the coronal loops in that region that otherwise would emit strongly in 171 A. Those low-lying coronal loops do not emit in 171 A because hot emission in loops of any length confined to low-enough heights is not allowed due to the thermal instability pointed out by Antiochos et al 1986.

Conclusions

- We have examined the dark moats frequently seen to surround ARs in AIA EUV coronal images, especially in emission from plasma at temperature near 1 MK.
- In our seven selected cases, we found that these dark moats vary in size and shape but are present in all our cases.
- Using DEM analysis, we found that in these moat regions, there is a dearth of emission at temperatures centered around 0.6--1.1 MK. Since the 171 A channel of AIA is most sensitive in this temperature range, the dark moats are most pronounced in the AIA 171 A images.
- By looking at the magnetic pressure distribution around the ARs using PFSS solutions, we find plausible the idea that these dark moats are a collateral consequence of the splay of strong loop magnetic field that extends out from the strong and concentrated magnetic flux of the AR.

References

- Antiochos, S. K., & Noci, G. 1986, ApJ, 301, 440, doi: 10.1086/163912
- Boerner, P., Edwards, C., Lemen, J., et al. 2012, Solar Physics, 275, 41, doi: 10.1007/s11207-011-9804-8
- Garton, T. M., Gallagher, P. T., & Murray, S. A. 2018, Journal of Space Weather and Space Climate, 8, A02, doi: 10.1051/swsc/2017039
- Lemen, J. R., Title, A. M., Akin, D. J., et al. 2012, Solar Physics, 275, 17, doi: 10.1007/s11207-011-9776-8
- Pesnell, W. D., Thompson, B. J., & Chamberlin, P. C. 2012, Solar Physics, 275, 3, doi: 10.1007/s11207-011-9841-3
- Schatten, K. H., Wilcox, J. M., & Ness, N. F. 1969, SoPh, 6, 442, doi: 10.1007/BF00146478
- Schrijver, C. J., & De Rosa, M. L. 2003, Solar Physics, 212, 165, doi: 10.1023/A:1022908504100
- Singh, T., Sterling, A. C., & Moore, R. L. 2021, ApJ, 909, 57, doi: 10.3847/1538-4357/abd7f2
- Withbroe, G. L. 1978, ApJ, 225, 641, doi: 10.1086/156524

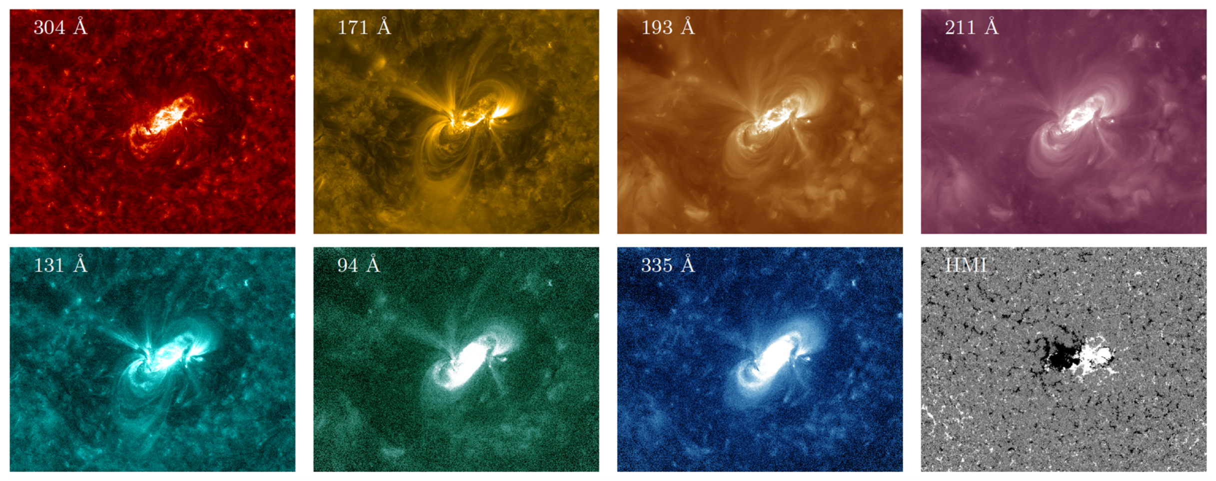

Figure 1: The active region of NOAA AR12699, from 2018 Feb 11 06:04 UT (Table 1 case 1), in seven SDO/AIA EUV channels and an HMI magnetogram. The cutout size is 840x660. The dark moat-like region around the AR is most obvious in the 171 A image, which has the strongest response to emissions over the temperature range 0.6-1.1 MK.

Table 1. Cases discussed in this study.

Case #	Date[a]	NOAA AR
1	2018 Feb 11	12699
2	2018 Apr 25	12706
3	2018 May 30	12712
4	2018 Jun 17	12713
5	2018 Jul 14	Unnumbered[b]
6	2019 Feb 20	Unnumbered[c]
7	2019 Apr 15	12704

Notes:

[a]The time for each case is 06:04 UT.

[b]Previous Carrington rotation AR number: 12713.

[c]Previous Carrington rotation AR number: 12733.

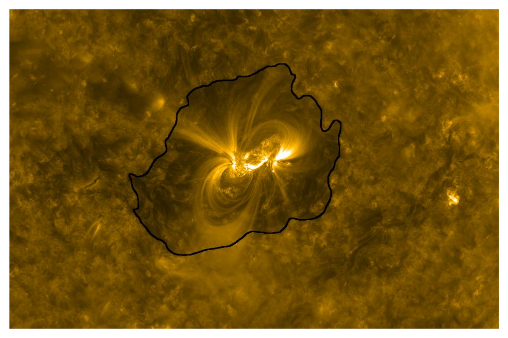

Figure 2: An SDO/AIA 171 A image cutout from 2018 Feb 11 at 06:04 UT; case 1 of Table 1. The cutout size is 1380x900. We have visually drawn a black boundary of the outer edge of the dark moat region.

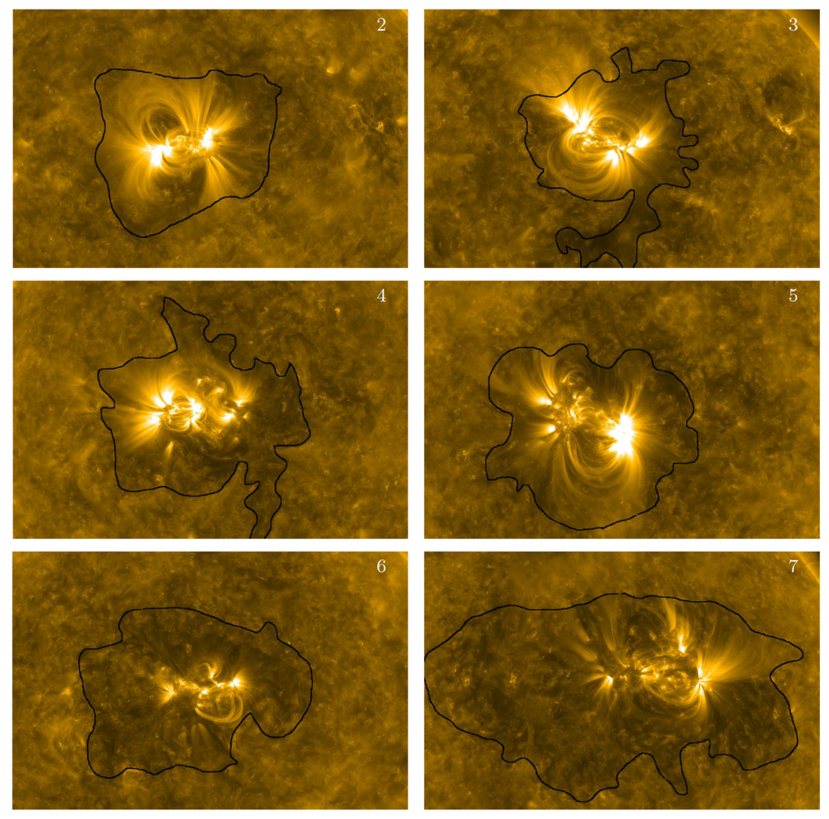

Figure 3: Similar to Fig. 1, but for Table 1 cases 2 to 7. The case number for each appears in the panels, and the dates and times are those listed in Table 1 for the respective case.

Table 2. Average emissions in different AIA wavelength measurements for all seven cases, along with the standard deviation across these cases.

Wavelength (Å)	Non-Moat (DN)	Moat (DN)	Relative Emission[a]
304	8.1 ± 0.3	7.3 ± 0.6	0.90 ± 0.09
171	212.6 ± 12.2	136.5 ± 23.1	0.64 ± 0.09
193	138.9 ± 13.4	178.5 ± 25.4	1.28 ± 0.26
211	41.0 ± 6.1	67.4 ± 8.0	1.64 ± 0.29
131	5.8 ± 0.1	4.4 ± 0.4	0.76 ± 0.07
94	0.9 ± 0.1	0.9 ± 0.1	0.96 ± 0.13
335	0.9 ± 0.1	1.0 ± 0.1	1.13 ± 0.15

Notes:

[a]Moat Emission/Non-Moat (quiet Sun) Emission. Standard deviation of this ratio is found using the Taylor expression of the second moment.

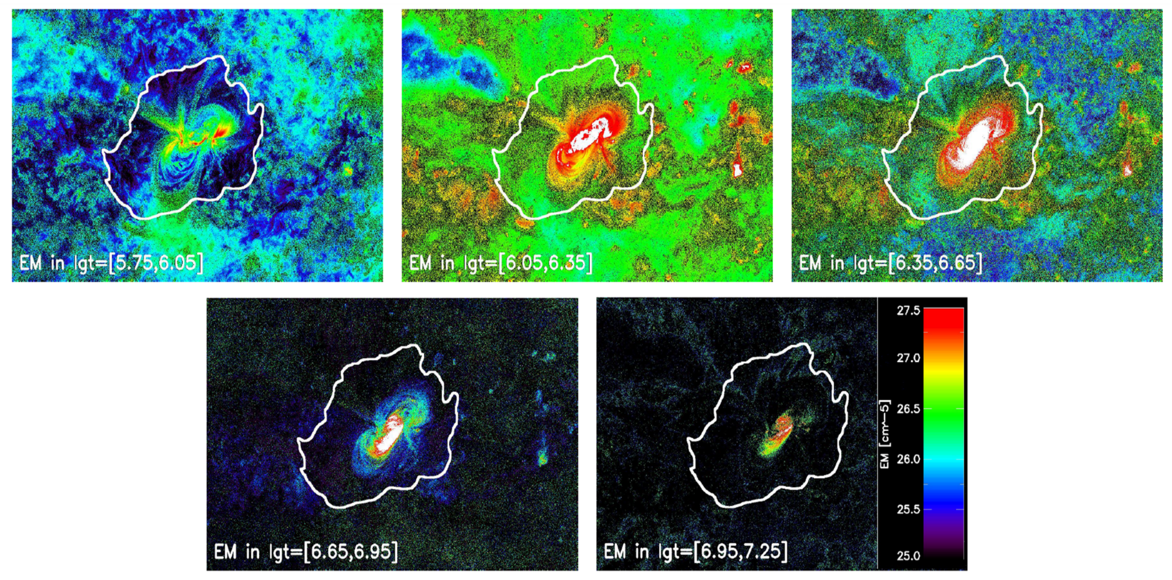

Figure 4: Emission measure (EM) maps of AR 12699 (Table 1 case 1), made using AIA 94, 131, 171, 193, 211, and 335 A images. We have visually drawn the boundary of the moat in the AIA 171 A image and overplotted it here as the white contour.

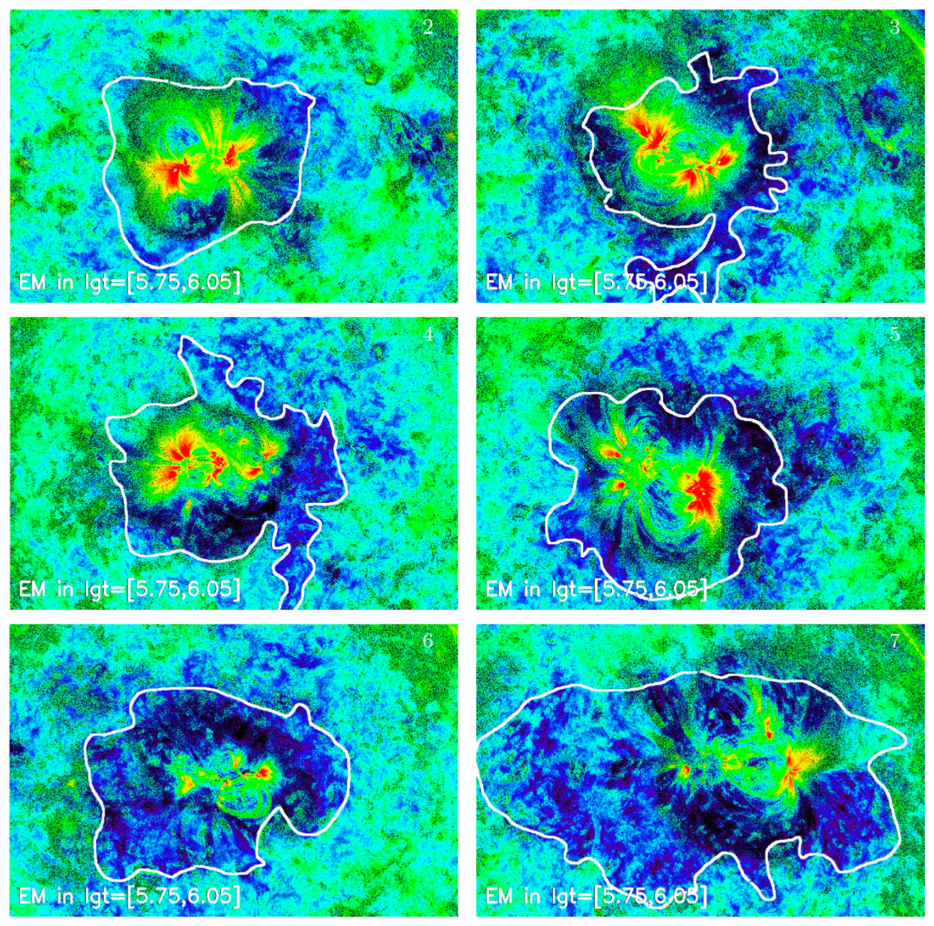

Figure 5: Similar to Fig. 4 but showing EM maps for Table 1 cases 2 to 7, showing EM in the log T range of 5.75 to 6.05, where the case numbers are indicated in the panels. Each case clearly shows low emission measure in the moat that appeared dark in the corresponding image in Fig. 2. This demonstrates that the moat-like dark regions around ARs are dark because they are deficient in plasma over this temperatures range. We have visually drawn the boundary of the moat in each AIA 171 A image in Fig. 3 and overplotted it here as the white contour.

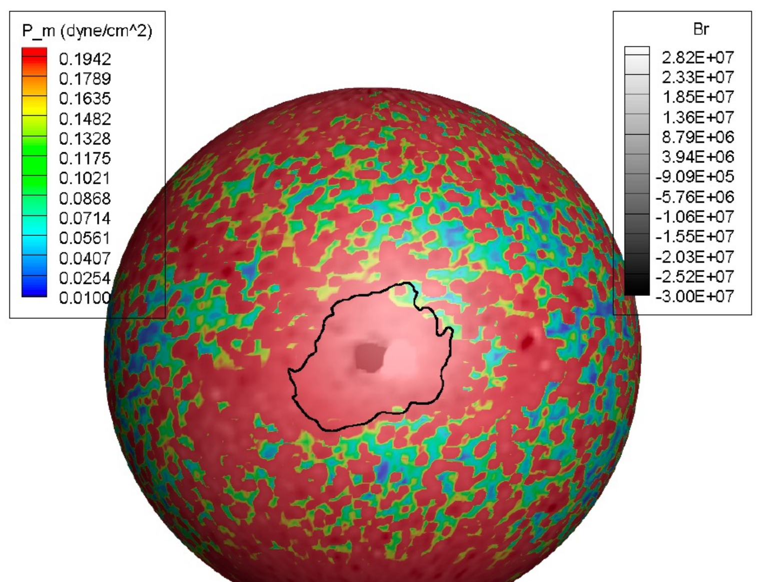

Figure 6: The magnetic pressure found using PFSS solution at 1.03 SR is shown using a semi translucent sphere for case 1 in Table 1. There is another sphere below this showing the synoptic magnetogram used to calculate the PFSS solution. The units of radial magnetic field Br in this graph are micro-Gauss. The visually found moat boundaries shown in Fig. 2 are over plotted on this sphere. The quiet sun magnetic pressure seems randomly distributed between 0.01 and 0.2 dyne/cm^2, but the region in the vicinity of the AR has magnetic pressure exceeding 0.2 dyne/cm^2. The moat boundaries roughly lie where we start observing regions with magnetic pressure less than 0.2 dyne/cm^2, while moving away from the AR.

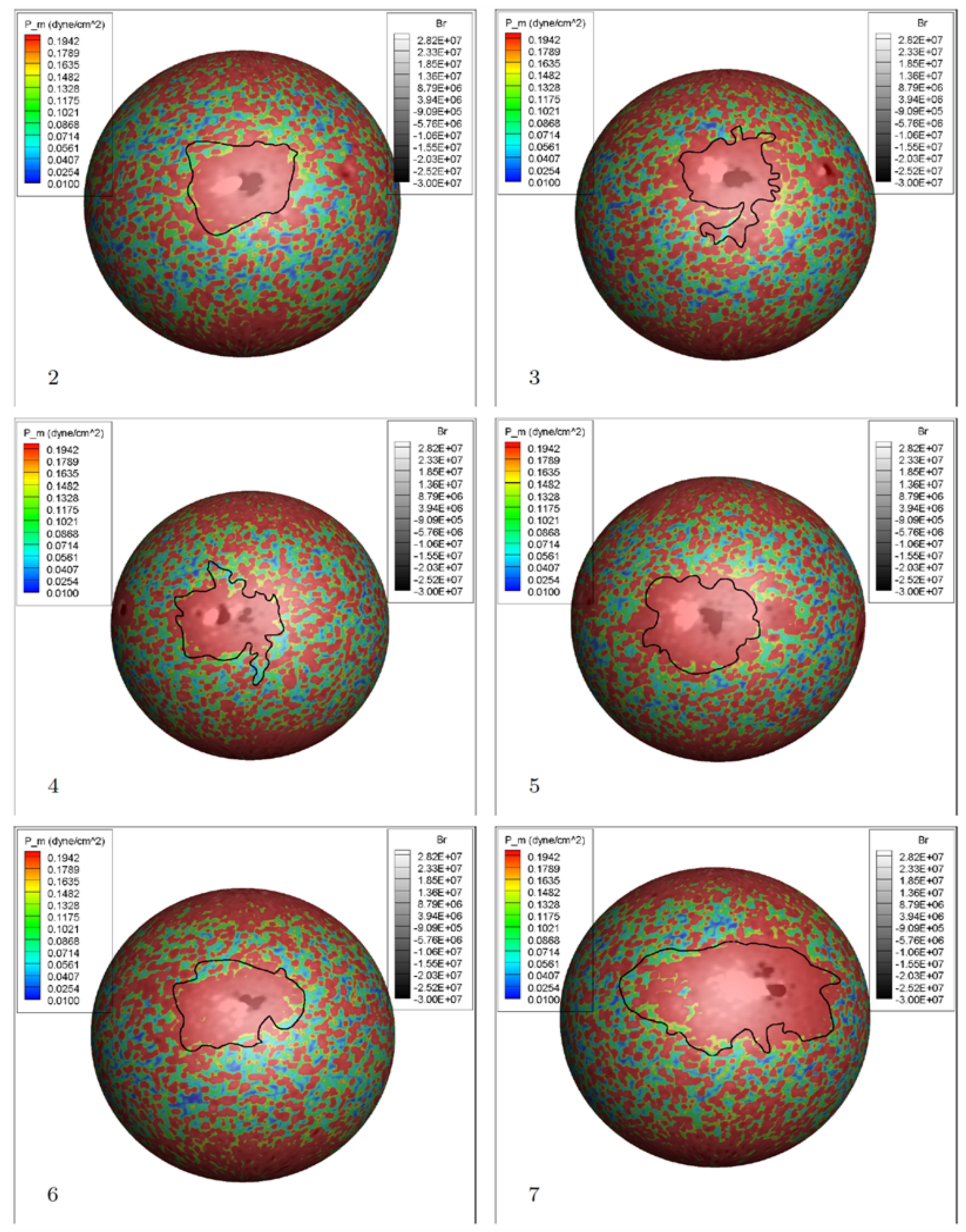

Figure 7: Similar to Figure 6, for cases 2-7 in Table 1.